Guidelines for MOSFET Device Optimization accounting for L-dependent Mobility Degradation

Grégory Bidal, Dominique Fleury, Gérard Ghibaudo, Frédéric Boeuf, Thomas Skotnicki

Guidelines for MOSFET Device Optimization accounting for L-dependent Mobility Degradation

G. Bidal[1,2], D. Fleury[1,2], G. Ghibaudo[2], F. Boeuf[1] and T. Skotnicki[1]

[1] STMicroelectronics, 850 rue Jean Monnet, 38926 Crolles, France ; [2] IMEP-LAHC, 3 Parvis Louis Néel, 38016 Grenoble, France
Tel: +33 438-92-3688, Fax: +33 438-92-3790, Email: frederic.boeuf@st.com

Abstract

This paper reports a new methodology to monitor L-dependent mobility degradation based on empirical modeling of experimental results. This method allows benchmarking the impact on mobility degradation of different technological modules, thus giving some guidelines for device optimization.

Introduction

As channel length L of MOSFETs is scaling down, carriers' mobility μ is degraded by additional scattering mechanisms with a dramatic impact below 100nm. As reported by Andrieu *et al.* [1] and by Cros *et al.* [2] (Fig.1), this mobility crisis affects both electrons and holes. Moreover, this degradation has been measured for both poly-Si gate and metal gate [3], for both high-K and SiO$_2$ [4], for strained and unstrained devices [1,3], for doped and undoped channel [2,4] and also whatever the device architecture: Bulk [1], SOI, [4,5], Gate-All-Around [2] or FinFET [6]. This μ(L) degradation was confirmed whatever the extraction method, i.e. Y-function, Split-CV or magneto-resistance [7], and cannot be solely explained by ballistic effects [8,9]. Unfortunately, mobility falls is a sign of a poor quality of the transport in the channel keeping us away from the ballistic regime. Whatever the conduction regime (ballistic or drift-diffusion), the on-state current will be limited by a maximum velocity that can be expressed as v$_{lim}$ = min(v$_{sat}$,v$_{inj}$) [10]. As shown in Fig.2, strong mobility degradation on short devices prevents from reaching the velocity limit, i.e. maximum on-current. Some authors [7,11] have identified those additional scattering mechanisms as impurity Coulomb scattering while neutral defects have been suggested by others [2,4]. This statement gives ground for a systematic examination of μ(L) degradation in order to establish guidelines for device optimization even if the precise origin of those additional scattering mechanisms is still not fully understood.

Extraction Methodology & μ-Degradation Modeling

A handy tool for extracting the mobility and monitoring its length dependence is the low field mobility $\mu_0 = \mu_{eff}(Q_{inv} \approx 0) = \beta_0 C_{ox}^{-1} L_{eff} W_{eff}^{-1}$. β_0 at low V$_{DS}$ (<<V$_{Dsat}$) is extracted from the Y-function [12] $Y(V_{GS}) = I_D/g_m^{1/2}$ while effective channel length and width (resp. L$_{eff}$ and W$_{eff}$) and gate oxide capacitance C$_{ox}$ are obtained independently from gate-to-channel C$_{GC}$(V$_{GS}$) measurements [13]. The notion of μ$_0$ is illustrated by Fig.3. It is also worth noticing that classical Coulomb scattering and surface roughness terms do not significantly alter μ$_0$ at 300K. Using first order θ$_1$ and second order θ$_2$ mobility attenuation parameters, μ$_{eff}$ in strong inversion can be reconstructed, showing good agreement in Fig.4 with R$_{SD}$-corrected split C-V extraction [14]. The use of μ$_0$ as a mobility indicator has been validated in Fig.5 by comparing it to split C-V extraction for different L$_{eff}$, clearly showing that μ$_0$ and μ$_{eff}$ are degraded in similar way as L$_{eff}$ is reduced. All our μ$_0$ extraction have been performed vs. L$_{eff}$ to fairly compare the different technological splits. In order to construct our guidelines, we have introduced a new length dependent mobility degradation fitting model: $1/\mu_0(L_{eff}) = 1/\mu_{max} + \alpha_\mu/L_{eff}$. The two fitting parameters are the maximum mobility μ$_{max}$ [cm^2.V^{-1}.s^{-1}], which is generally equal to the "long" channel mobility, and a mobility degradation factor α$_\mu$ [nm.V.s.cm^{-2}]. Fig.6 illustrates the different kinds of μ$_0$(L$_{eff}$) curves that can be obtained, α$_\mu$=0 meaning zero degradation and thus a constant μ$_0$. However, it should be noted that α$_\mu$ cannot be lower than its minimum value given by the ballistic mobility [15] $\alpha_{\mu bal} = (2kT/q)/v_{inj}$, v$_{inj}$ being the injection velocity at source (α$_{\mu bal}$ =0.04 or 0.08 nm.V.s.cm^{-2} for electron and hole respectively).

Experimental Results

Gate stack: Gate stack impact on μ$_0$ was examined in Fig.7 & Fig.8. In Fig.7, two plasma nitrided SiON gate oxide thicknesses (12Å vs. 17Å) were compared for the same poly-Si gate, showing more degraded electron mobility for the thinner 12Å oxide. In Fig.8, we have found that nitrided metal gates (TiN, TaN) lead to more degraded electron mobility than the non-nitrided TaC metal gate. Those results are suggesting that N-species in the gate oxide and/or in the gate electrode lead to a lower long channel mobility in agreement with [16], but also to a higher α$_\mu$ i.e. to stronger scattering mechanisms.

Channel doping: Effect of channel doping was examined in Fig.9 using ultra thin body (UTB) structures in both cases (doped vs. undoped) for avoiding short channel effects disturbances. Devices fabricated using Silicon-On-Nothing (SON) technology have bulk S/D [17]. We found that increasing the channel doping is lowering the long channel electron mobility but has no significant effect on additional scattering mechanisms since close α$_\mu$ values were found.

Junction architecture: Since neutral defects introduction is likely related to the junction (S/D+LDD) ion implantation (I/I), S/D architecture appears as a key module for improving mobility degradation. Cros *et al.* have already shown in [2] that an increase of the temperature during the RTP activation anneal could cure partially the mobility degradation. Taking the problem differently, we have examined if it was possible to improve mobility degradation by changing I/I conditions (species, energy, dose). Results in Fig. 10 are demonstrating that S/D architecture optimization is possible even when reducing the RTP temperature.

Mobility boosters: After having examined some possible causes of degradation, we have now investigating the effects of mobility boosters on mobility degradation. Local process induced stress (PIS) engineering by using eSiGe stressors is studied in Fig.11, while surface orientation is considered in Fig.12. Even if both strategies have an impact on holes' μ$_{max}$, only local PIS which is also L-dependent [18] significantly improves α$_\mu$.

Discussion & Guidelines

Seeing the strong degradation of the mobility, one could think that any mobility improvement is not relevant since all strategies will finally have the same mobility at very short gate length. Using our model, we have extrapolated from the measurements the resulting mobility at L$_{eff}$=10nm in Fig.13. We can see that mobility improvement is still possible even at 10nm if well optimized. We have also investigated a possible link between μ$_{max}$ and α$_\mu$ in Fig.14: no clear correlation was found between the two parameters meaning that they are needed to monitor the mobility degradation. Thus we have introduced a new figure of merit η=μ$_{max}$/ α$_\mu$. Higher η is, higher the short channel mobility will be and closer to its limiting velocity the device will operate. Finally, we give some guidelines, based on this work in Fig.15 in order to limit μ(L) degradation.

Conclusion

Using a new monitoring method based on empirical modeling of μ(L) degradation, we have systematically examined the impact on μ(L) of the gate stack, channel doping, junction architecture and mobility boosters. It has been found that this degradation is not ineluctable and that working on key technological modules would help us to get closer to the ballistic regime.
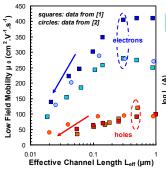
Acknowledgments

Fig.1: Literature data from [1] & [2] clearly showing length dependent mobility degradation for both electrons and holes.

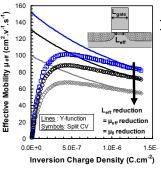Fig.2: Strong mobility degradation on short devices prevents from reaching the velocity limit, i.e. maximum on-current.

In Fig.2: $I_{dd} = \mu_{eff} C_{ox} \frac{W}{L} V_{gt}^2$; Mobility limit ; Velocity limit ; $I_{sat} = W C_{ox} V_{gt} v_{lim}$; Additional mobility degradation on short devices ; Same long channel mobility. N.B. : limiting velocity v_{lim} stands for v_{sat} in drift-diffusion transport and for v_{inj} in ballistic transport

Fig.3: Illustration of low field mobility $\mu_0 = \mu(Q_{inv} \approx 0)$. Coulomb scattering & surface roughness limitations are negligible.

In Fig.3: Low field mobility μ_0 measured by Y-function @$Q_{inv} \sim 0$; Phonon scattering θ_1 ; Surface roughness scattering θ_2 ; Total mobility without Coulomb scattering limitation. N.B. :Low field mobility μ_0 is measured at low V_{DS} ($<<V_{Dsat}$)

Fig.4: Series resistance R_{SD} correction which is critical on short devices is intrinsically taken into account when using Y-function.

In Fig.4: μ_0 ; Y-function model: $\mu_{eff} = \dfrac{\mu_0}{1 + \theta_1 V_{gt} + \theta_2 V_{gt}^2}$; split CV with R_{SD} correction ; split CV without R_{SD} correction ; $L_{eff} = 46nm$

Fig.5: μ_{eff} measurements for different L_{eff}. θ_1 and θ_2 are kept constant for all channel lengths. Inset: L_{eff} definition.

In Fig.5: L_{gate} ; L_{eff} ; Lines : Y-function, Symbols: Split CV ; L_{eff} reduction = μ_{eff} reduction = μ_0 reduction

Fig.6: Length dependent mobility degradation model introducing mobility degradation factor α_μ. For $\alpha_\mu = 0$, $\mu_0(L_{eff}) = Cte$.

In Fig.6: Model: $1/\mu_0(L_{eff}) = 1/\mu_{max} + \alpha_\mu / L_{eff}$; $\mu_{max} = \mu_{long} = 400$; $\mu_{max} = \mu_{long} = 300$; $\mu_{max} = \mu_{long} = 200$; $\alpha_\mu = 0$; $\alpha_\mu = 0.05$; $\alpha_\mu = 0.1$; $\alpha_\mu = 1$

Fig.7: Comparison of electron mobility between two SiON gate oxide thicknesses. Thinner 12Å oxide is more degraded than 17Å.

In Fig.7: symbols: measured, lines: model ; poly-Si Gate ; 17Å-SiON ; Si channel ; $\alpha_\mu = 0.15$ $\mu_{max} = 400$; nMOS ; $\alpha_\mu = 0.25$ $\mu_{max} = 290$; poly-Si Gate ; 12Å-SiON ; Si channel

Fig.8: Comparison of electron mobility between different metal gate materials. Nitrided metals are more degraded than not nitrided.

In Fig.8: symbols: measured lines: model ; $\alpha_\mu = 0.18$ $\mu_{max} = 360$; nMOS ; $\alpha_\mu = 0.28$ $\mu_{max} = 300$; TaC gate ; TaN gate ; TiN gate
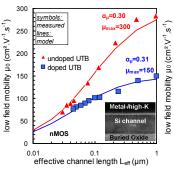
Fig.9: Comparison of electron mobility between undoped & doped ultra thin body (UTB) with high-K/metal gate stack.

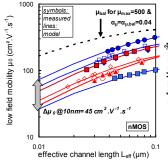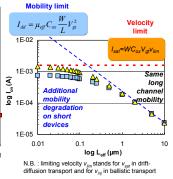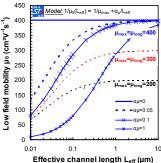In Fig.9: symbols: measured lines: model ; $\alpha_\mu = 0.30$ $\mu_{max} = 300$; undoped UTB ; doped UTB ; $\alpha_\mu = 0.31$ $\mu_{max} = 150$; Metal /high-K ; Si channel ; Buried Oxide ; nMOS
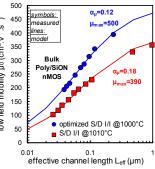
Fig.10: Comparison of electron mobility between two S/D architectures while keeping the same Poly/SiON gate stack.

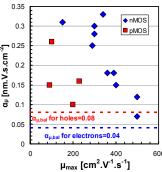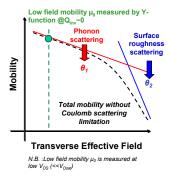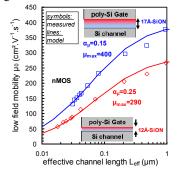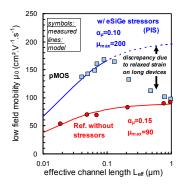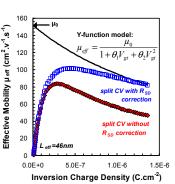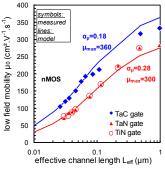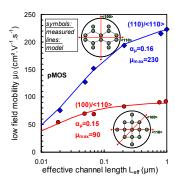In Fig.10: symbols: measured lines: model ; $\alpha_\mu = 0.12$ $\mu_{max} = 500$; Bulk Poly/SiON nMOS ; $\alpha_\mu = 0.18$ $\mu_{max} = 390$; optimized S/D I/I @1000°C ; S/D I/I @1010°C

Fig.11: Comparison of hole mobility between unstrained reference and locally strained device with eSiGe S/D stressors.

In Fig.11: symbols: measured lines: model ; w/ eSiGe stressors (PIS) $\alpha_\mu = 0.10$ $\mu_{max} = 200$; discrepancy due to relaxed strain on long devices ; pMOS ; Ref. without stressors ; $\alpha_\mu = 0.15$ $\mu_{max} = 90$

Fig.12: Comparison of hole mobility between (100)/<110> device and (110)/<110> device with same poly/SiON gate stack.

In Fig.12: symbols: measured lines: model ; (110)/<110> ; $\alpha_\mu = 0.16$ $\mu_{max} = 230$; pMOS ; (100)/<110> ; $\alpha_\mu = 0.15$ $\mu_{max} = 90$

Fig.13: Sub-100nm electron mobility with extrapolation at $L_{eff} = 10nm$ using our model.

In Fig.13: symbols: measured lines: model ; μ_{bal} for $\mu_{max} = 500$ & $\alpha_\mu = \alpha_{\mu,bal} = 0.04$; $\Delta\mu_0$ @10nm= 45 cm^2.V^{-1}.s^{-1} ; nMOS

Fig.14: α_μ as a function of μ_{max} clearly showing no universal correlation between α_μ & μ_{max}.

In Fig.14: nMOS ; pMOS ; $\alpha_{\mu,bal}$ for holes=0.08 ; $\alpha_{\mu,bal}$ for electrons=0.04

Fig.15: Guidelines for short channel mobility optimization based on the figure of merit $\eta = \mu_{max} / \alpha_\mu$.

Techno. module	impact on μ_{max}	impact on α_μ	η
Gate stack	+	++	x2 to x4
Junctions	+	+	x2
Channel doping	++	=	x2
Local PIS	++	+	x3
Crystal orientation	++	=	X2

References

[1] F.Andrieu *et al.*, VLSI 2005. [2] A.Cros *et al.*, IEDM 2006. [3] G.Bidal *et al.*, SSDM 2008. [4] L.Pham-Nguyen *et al.*, SOI conf. 2008. [5] C.Gallon et al., SOI conf. 2005. [6] J.Ramos *et al.*, ESSDERC 2006. [7] M.Cassé *et al.*, VLSI 2008. [8] M.Zilli *et al.*, EDL, v.28, Issue 11, 2007. [9] I.Pappas *et al.*, SSE, v.53, 2009. [10] D.Fleury *et al.*, submitted to VLSI 2009. [11] V.Barral *et al.*, SNW 2008. [12] G. Ghibaudo *et al.*, Elec. Let., v.24, 1988. [13] D.Fleury *et al.*, TSM, v. 21, Issue 4, 2008. [14] K. Romanjek *et al.*, EDL, v.25, 2004. [15] M.Shur *et al.*, EDL, v23, 2002. [16] X.Garros *et al.*, VLSI 2008. [17] G.Bidal *et al.*, VLSI 2008. [18] F.Payet *et al.*, TED v. 55, Issue 4, 2008.